MOX–Report No. 42/2011

Numerical performance of discontinuous and stabilized continuous Galerkin methods or convection-diffusion problems

Antonietti, P.F.; Quarteroni, A.

MOX, Dipartimento di Matematica "F. Brioschi"
Politecnico di Milano, Via Bonardi 9 - 20133 Milano (Italy)

mox@mate.polimi.it http://mox.polimi.it

Numerical performance of discontinuous and stabilized continuous Galerkin methods for convection–diffusion problems

Paola F. Antonietti[♮], Alfio Quarteroni[♮,♭]

November 27, 2011

[♮] MOX, Dipartimento di Matematica, Politecnico di Milano, Piazza Leonardo da Vinci 32, 20133 Milano, Italy
paola.antonietti@polimi.it

[♭] CMCS, Ecole Polytechnique Federale de Lausanne (EPFL), Station 8, 1015 Lausanne, Switzerland
alfio.quarteroni@epfl.ch

Abstract

We compare the performance of two classes of numerical methods for the approximation of linear steady–state convection–diffusion equations, namely, the discontinuous Galerkin (DG) method and the continuous streamline upwind Petrov-Galerkin (SUPG) method. We present a fair comparison of such schemes considering both diffusion–dominated and convection–dominated regimes, and present numerical results obtained on a series of test problems including smooth solutions, and test cases with sharp internal and boundary layers.

1 Introduction

Convection–diffusion equations occur in the mathematical modeling of a wide range of phenomena as semiconductor devices modeling, magnetostatics and electrostatic flows, heat and mass-transfer, and flows in porous media related to oil and groundwater applications. The linear steady–state convection–diffusion equation with constant coefficients posed on a domain $\Omega \subseteq \mathbb{R}^d$, $d = 2, 3$, is a boundary value problem of the form

$$\begin{aligned} -\varepsilon \Delta u + \mathrm{div}(\boldsymbol{\beta} u) &= f \quad \text{in } \Omega, \\ u &= 0 \quad \text{on } \partial\Omega, \end{aligned} \tag{1}$$

where $f \in L^2(\Omega)$ is a given real-valued function, $\varepsilon > 0$ is the diffusion parameter and $\boldsymbol{\beta} \in \mathbb{R}^d$, $d = 2, 3$, represents a constant (for simplicity) velocity field. In many physical phenomena the convection has much greater magnitude than the diffusion, i.e., $\|\boldsymbol{\beta}\|/\varepsilon \gg 1$. In such cases, problem (1) is an example of a singularly perturbed problem (with respect to ε): that is, the solution in the case $\varepsilon = 0$ (with boundary conditions prescribed not on the whole boundary $\partial\Omega$ but

on $\partial\Omega_{\text{in}} = \{x \in \partial\Omega : \boldsymbol{\beta} \cdot \boldsymbol{n}(x) < 0\}$ with $\boldsymbol{n}(x)$ denoting the unit outward normal vector to $\partial\Omega$ at the point $x \in \partial\Omega$, see (2) below) is not equal, at all points, to the limit of the solutions as $\varepsilon \searrow 0^+$. From the numerical viewpoint, the design of robust numerical schemes for the solution of (1) represents a challenging problem, and indeed there has been an extensive development of discretizations methods for convection–diffusion equations that are robust in all the regimes, see [26], for example (cf. also [14, 21, 20]). Among the numerical methods developed so far, we are interest here in discontinuous and stabilized continuous Galerkin finite element methods which restore two opposite paradigms within the finite element approach, namely non-conforming (discontinuous) versus conforming (continuous) approximation spaces.

Stabilized conforming finite element methods have been extensively developed for hyperbolic and parabolic conservation laws. The original conforming stabilized method for advection-diffusion equations, the Streamline-Upwind Petrov-Galerkin (SUPG), was developed by [8] and then analyzed by [19] (see also [10] for the analysis of the SUPG method for transient convection-diffusion equations). It provides an upwinding effect to standard finite element methods using the Petrov-Galerkin framework. It is well known that the SUPG method has the capability of improving numerical stability for convection–dominated flows, while satisfying a strong consistency property. Like many other conforming stabilized methods, the SUPG scheme contains an elementwise stabilization parameter τ that has to be tuned in practice, and, except for simplified situations, the "optimal" value is not known. More precisely, for linear finite element discretizations of a one-dimensional problem with constant coefficients $\varepsilon \in \mathbb{R}^+$, $\beta \in \mathbb{R}$ and constant data it can be shown that the choice

$$\tau = \frac{h}{2\,|\beta|}\left(\coth(\mathsf{Pe}_T) - \frac{1}{\mathsf{Pe}_T}\right),$$

where Pe_T is the mesh Péclet number (cf. also (5), below), leads to a nodally exact approximate solution [8], see also [11]. In the multidimensional case, many different choices of the stabilization parameter τ have been proposed see [15], and the references therein. It is also known that the choice of the stabilization parameter τ also influences the behavior of the iterative solvers employed to solve the resulting linear system of equations. For example, GMRES converges more slowly for worse stabilization parameters, as pointed out in [22].

On the other hand, discontinuous Galerkin (DG) methods are parameters free since they do not rely on the addiction of *ad-hoc tuned* streamline stabilization terms. Since their introduction in 1970s [25, 13, 3], the discontinuous Galerkin method has become a topic of extensive research for the numerical solution of differential equations. DG methods employ piecewise polynomial spaces which may be discontinuous across elements boundaries. Therefore, DG can accommodate non-matching meshes as well as variable polynomial approximation orders. These features make them ideally suited for both geometrical and functional adaptive discretizations. Moreover, DG methods are locally mass conservative and can capture possible discontinuities in the solution thanks to the discontinuous approximation spaces. For such capabilities, DG methods have been extensively developed for convection–diffusion problems, cf. for example [12, 6, 16, 9, 1, 5], and the references therein.

In this paper we aim at comparing DG and SUPG solutions, working, for the sake of simplicity, on a linear steady–state convection–diffusion equation with constant coefficients. A detailed assessment of the performance of such schemes (employing the lowest order elements) with respect to accuracy is presented in a number of test problems featuring smooth solutions, and other problems featuring sharp layers (either internal or boundary's).

The rest of the paper is organized as follows. In Section 2 we introduce some notation and recall the variational formulation of problem (1). In Section 3 and Section 4 we recall the DG and SUPG formulations and the corresponding error estimates, respectively. Section 4 contains an extensive set of numerical experiments to compare the DG and SUPG solutions. Finally, in Section 6 we draw some conclusions.

2 Model problem

We consider the linear steady–state convection–diffusion equation with constant coefficients (1) posed on Ω, a bounded convex open polygonal (resp. polyhedral) domain in $\mathbb{R}^2$ (resp. $\mathbb{R}^3$). The corresponding weak formulation reads as: Find $u \in H_0^1(\Omega)$ such that

$$\int_\Omega (\varepsilon \nabla u - \boldsymbol{\beta} u) \cdot \nabla v \, \mathrm{dx} = \int_\Omega f v \, \mathrm{dx} \quad \forall v \in H_0^1(\Omega).$$

The existence of a unique solution of the above problem follows from the Lax-Milgram Theorem. For the analysis of more general convection–diffusion equations see, e.g., [24]. For the design and analysis of DG methods in the case of a diffusion tensor whose entries are bounded, piecewise continuous real-valued functions defined on $\overline{\Omega}$ and a piecewise continuous real-valued velocity field, we refer to [5]. By $\boldsymbol{n} \equiv \boldsymbol{n}(x)$ we denote the unit outward normal vector to $\partial\Omega$ at the point $x \in \partial\Omega$, and define the sets $\partial\Omega_{\mathrm{in}}$ and $\partial\Omega_{\mathrm{out}}$ of inflow and outflow boundary, respectively, as

$$\begin{aligned} \partial\Omega_{\mathrm{in}} &= \{x \in \Gamma : \boldsymbol{\beta} \cdot \boldsymbol{n} < 0\}, \\ \partial\Omega_{\mathrm{out}} &= \{x \in \Gamma : \boldsymbol{\beta} \cdot \boldsymbol{n} \geq 0\}. \end{aligned} \tag{2}$$

3 DG and SUPG discretisations

The aim of this section is to introduce the DG and SUPG discretisations.

Let $\mathcal{T}_h$ be a conforming shape-regular quasi-uniform partition of Ω into disjoint open triangles T where each $T \in \mathcal{T}_h$ is the affine image of the reference open unit d-simplex in $\mathbb{R}^d$, $d = 2, 3$. Denoting by h_T the diameter of an element $T \in \mathcal{T}_h$, we define the mesh size $h = \max_{T \in \mathcal{T}_h} h_T$.

3.1 The DG method

We start by introducing suitable trace operators, defined in the usual way [4]. Let $\mathcal{F}_h^I$ and $\mathcal{F}_h^B$ be the sets of all the interior and boundary $(d-1)$-dimensional (open) faces (if $d = 2$, "face" means "edge"), respectively, we set $\mathcal{F}_h = \mathcal{F}_h^I \cup \mathcal{F}_h^B$. We also decompose $\mathcal{F}_h^B = \mathcal{F}_h^{B_{\mathrm{out}}} \cup \mathcal{F}_h^{B_{\mathrm{in}}}$, where $\mathcal{F}_h^{B_{\mathrm{out}}} = \{F \in \mathcal{F}_h^B : F \subset \partial\Omega_{\mathrm{out}}\}$ and

$\mathcal{F}_h^{B_{\rm in}} = \{F \in \mathcal{F}_h^B : F \subset \partial\Omega_{\rm in}\}$. Implicit in these definitions is the assumption that $\mathcal{T}_h$ respects the decomposition of $\partial\Omega$in the sense that each $F \in \mathcal{F}_h$ that lies on $\partial\Omega$belongs to the interior of exactly one of $\partial\Omega_{\rm out}$, $\partial\Omega_{\rm in}$. Let $F \in \mathcal{F}_h^I$ be an interior face shared by the elements T^+ and T^- with outward unit normal vectors $\boldsymbol{n}^+$ and $\boldsymbol{n}^-$, respectively. For piecewise smooth vector–valued and scalar functions $\boldsymbol{\tau}$ and z, respectively, let $\boldsymbol{\tau}^\pm$ and $z^\pm$ be the traces of $\boldsymbol{\tau}$ and z on $\partial T^\pm$ taken within the interior of $T^\pm$, respectively. We define the *jump* and the *average* across F by

$$\begin{aligned} [\![\boldsymbol{\tau}]\!] &= \boldsymbol{\tau}^+ \cdot \boldsymbol{n}^+ + \boldsymbol{\tau}^- \cdot \boldsymbol{n}^-, \qquad [\![z]\!] = z^+\boldsymbol{n}^+ + z^-\boldsymbol{n}^-, \\ \{\!\{\boldsymbol{\tau}\}\!\} &= (\boldsymbol{\tau}^+ + \boldsymbol{\tau}^-)/2, \qquad\quad \{\!\{z\}\!\} = (z^+ + z^-)/2. \end{aligned}$$

On a boundary face $F \in \mathcal{F}_h^B$, we set, analogously,

$$[\![z]\!] = z\,\boldsymbol{n}, \quad \{\!\{\boldsymbol{\tau}\}\!\} = \boldsymbol{\tau}.$$

We do not need either $[\![\boldsymbol{\tau}]\!]$ or $\{\!\{v\}\!\}$ on boundary faces, and leave them undefined. On each interior face $F \in \mathcal{F}_h^I$, we introduce an *upwind* average $\{\!\{\cdot\}\!\}_{\boldsymbol{\beta}}$ defined as

$$\{\!\{\boldsymbol{\beta}u\}\!\}_{\boldsymbol{\beta}} = \begin{cases} \boldsymbol{\beta}u^+ & \text{if } \boldsymbol{\beta}\cdot\boldsymbol{n}^+ > 0 \\ \boldsymbol{\beta}u^- & \text{if } \boldsymbol{\beta}\cdot\boldsymbol{n}^+ < 0 \\ \boldsymbol{\beta}\,\{\!\{u\}\!\} & \text{if } \boldsymbol{\beta}\cdot\boldsymbol{n}^+ = 0 \end{cases}$$

On $F \in \mathcal{F}_h^B$, we set $\{\!\{\boldsymbol{\beta}u\}\!\}_{\boldsymbol{\beta}} = \boldsymbol{\beta}u$, if $\boldsymbol{\beta}\cdot\boldsymbol{n} > 0$, $\{\!\{\boldsymbol{\beta}u\}\!\}_{\boldsymbol{\beta}} = \mathbf{0}$ otherwise. For a given approximation order $\ell \geq 1$, we introduce the DG finite element space $V_h^{\rm DG}$ as

$$V_h^{\rm DG} = \{v \in L^2(\Omega) : v|_T \in \mathbb{P}^\ell(T) \quad \forall T \in \mathcal{T}_h\},$$

where $\mathbb{P}^\ell(T)$ is the set of polynomials of total degree ℓ on T.

We define the bilinear form $\mathcal{A}_h^{\rm DG}(\cdot,\cdot) : V_h^{\rm DG} \times V_h^{\rm DG} \longrightarrow \mathbb{R}$ as

$$\begin{aligned} \mathcal{A}_h^{\rm DG}(u,v) = &\sum_{T\in\mathcal{T}_h} \int_T (\varepsilon\nabla u - \boldsymbol{\beta}u)\cdot\nabla v \,\mathrm{dx} \\ &- \sum_{F\in\mathcal{F}_h} \int_F (\{\!\{\varepsilon\nabla u\}\!\}\cdot[\![v]\!] + [\![u]\!]\cdot\{\!\{\varepsilon\nabla v\}\!\})\,\mathrm{ds} \\ &+ \sum_{F\in\mathcal{F}_h} \int_F \left(\sigma_F\,[\![u]\!]\cdot[\![v]\!] + \{\!\{\boldsymbol{\beta}u\}\!\}_{\boldsymbol{\beta}}\cdot[\![v]\!]\right)\mathrm{ds} \end{aligned}$$

with the convention that the application of the operator ∇ has to be intendend elementwise whenever the function to which is applied is elementwise discontinuous. Here σ_F is defined for all $F \in \mathcal{F}_h$ as

$$\sigma_F = \alpha\frac{\varepsilon\ell^2}{h_F} \quad \forall F \in \mathcal{F}_h, \tag{3}$$

with α a positive real number at our disposal, and h_F the diameter of the face $F \in \mathcal{F}_h$. The DG approximation of problem (1) is defined as follows : find $u_h^{\rm DG} \in V_h^{\rm DG}$ such that

$$\mathcal{A}_h^{\rm DG}(u_h^{\rm DG}, v_h) = \int_\Omega f v_h \,dx \quad \forall v_h \in V_h^{\rm DG}.$$

Remark 3.1. *For the approximation of the convection and diffusion terms we have employed a DG method with upwinded fluxes [7] and the symmetric interior penalty (SIPG) method [3], respectively. With minor changes, any other (possibly unsymmetric) DG approximation of the second order term could be considered.*

We close this section observing that, denoting by $\boldsymbol{n}_F$ the normal to the face $F \in \mathcal{F}_h$, it holds

$$\sum_{F\in\mathcal{F}_h}\int_F \{\!\{\boldsymbol{\beta}u\}\!\}_{\boldsymbol{\beta}}\cdot[\![v]\!]\,\mathrm{ds} = \sum_{F\in\mathcal{F}_h^I\cup\mathcal{F}_h^{B_{\mathrm{out}}}}\int_F \{\!\{\boldsymbol{\beta}u\}\!\}\cdot[\![v]\!]\,\mathrm{ds} + \sum_{F\in\mathcal{F}_h^I}\int_F \frac{|\boldsymbol{\beta}\cdot\boldsymbol{n}_F|}{2}[\![u]\!]\cdot[\![v]\!]\,\mathrm{ds}\,,$$

for all $u, v \in V_h^{\mathrm{DG}}$. Therefore, the *upwind* value of $\boldsymbol{\beta}u$, can be written as the sum of the usual (symmetric) average plus a jump penalty term. Such equivalent representation has several advantages. For example, notice that both terms on the right hand side are of the same kind as the ones already present in the treatment of the diffusive part of the operator. This can be favorably exploited in the implementation process.

3.2 The SUPG method

Let the SUPG discrete space be defined as the subspace of V_h^{DG} of continuous polynomials that also satisfy the boundary condition, i.e.,

$$V_h^{\mathrm{SUPG}} = \{v \in C^0(\overline{\Omega}) : v|_T \in \mathbb{P}^\ell(T) \quad \forall T \in \mathcal{T}_h, \text{ and } v = 0 \text{ on } \partial\Omega\},$$

For piecewise positive parameters τ_T, we define the bilinear form $\mathcal{A}_h^{\mathrm{SUPG}}(\cdot,\cdot) : V_h^{\mathrm{SUPG}} \times V_h^{\mathrm{SUPG}} \longrightarrow \mathbb{R}$ as

$$\mathcal{A}_h^{\mathrm{SUPG}}(u,v) = \int_\Omega (\varepsilon\nabla u - \boldsymbol{\beta}u)\cdot\nabla v\,\mathrm{dx} + \sum_{T\in\mathcal{T}_h}\int_T \tau_T(-\varepsilon\Delta u + \boldsymbol{\beta}\cdot\nabla u)\boldsymbol{\beta}\cdot\nabla v\,\mathrm{dx}\,,$$

and the functional $\mathcal{F}_h^{\mathrm{SUPG}}(\cdot) : V_h^{\mathrm{SUPG}} \longrightarrow \mathbb{R}$

$$\mathcal{F}_h^{\mathrm{SUPG}}(v) = \sum_{T\in\mathcal{T}_h}\int_T f\,(v + \tau_T\boldsymbol{\beta}\cdot\nabla v)\,dx.$$

Here, for any $T \in \mathcal{T}_h$, τ_T is a non-negative constant stabilization parameter defined as

$$\tau_T = \frac{h_T}{2\|\boldsymbol{\beta}\|}\xi(\mathsf{Pe}_T), \tag{4}$$

with Pe_T being the local Péclet number, i.e.,

$$\mathsf{Pe}_T = \frac{\|\boldsymbol{\beta}\|h_T}{2\varepsilon}, \tag{5}$$

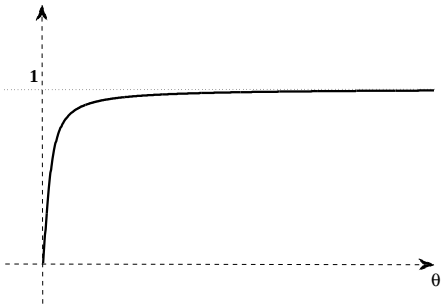

Figure 1: Stabilization function $\xi(\theta) = \coth(\theta) - 1/\theta$.

and where $\|\boldsymbol{\beta}\|$ is the Euclidean norm of $\boldsymbol{\beta}$, and $\xi(\cdot)$ is an upwind function defined as

$$\xi(\theta) = \coth(\theta) - 1/\theta, \quad \theta > 0,$$

cf. Figure 1. Notice that $\xi(\theta) \to 1$ for $\theta \to \infty$, and $\xi(\theta)/\theta \to 1/3$ for $\theta \to 0^+$ (and the SUPG stabilization is not necessary for $\theta \to 0^+$). We refer to [17, 18] for further details.

Then, the SUPG formulation reads: find $u_h^{\mathrm{SUPG}} \in V_h^{\mathrm{SUPG}}$ such that

$$\mathcal{A}_h^{\mathrm{SUPG}}(u_h^{\mathrm{SUPG}}, v_h) = \mathcal{F}_h^{\mathrm{SUPG}}(v_h) \quad \forall v_h \in V_h^{\mathrm{SUPG}}.$$

4 Error estimates

In this section we briefly recall the error estimates for the DG and SUPG formulations.

To deal with the convection–dominated regime, we first introduce a norm which controls the streamline derivative:

$$\|v\|_{\boldsymbol{\beta}} = \left(\sum_{T \in \mathcal{T}_h} \|\tau_T^{1/2} \boldsymbol{\beta} \cdot \nabla v\|_{0,T}^2 \right)^{1/2} \quad \forall v \in H^1(\mathcal{T}_h), \tag{6}$$

where τ is defined in (4), and where the piecewise broken Sobolev space $H^1(\mathcal{T}_h)$ consists of functions v such that $v|_T \in H^1(T)$ for any $T \in \mathcal{T}_h$. We endow the DG space with the norm

$$\|v\|_{\mathrm{DG}} = \left(|||v|||^2 + \|v\|_{\boldsymbol{\beta}}^2 \right)^{1/2} \quad \forall v \in V_h^{\mathrm{DG}}, \tag{7}$$

where $\|\cdot\|_{\boldsymbol{\beta}}$ is defined in (6), and where

$$|||v|||^2 = \sum_{T \in \mathcal{T}_h} \|\varepsilon^{1/2} \nabla v\|_{0,T}^2 + \sum_{F \in \mathcal{F}_h} \|\alpha_F^{1/2} [\![v]\!]\|_{0,F}^2$$

for all $v \in V_h^{\mathrm{DG}}$. Here α_F is defined as

$$\alpha_F = \sigma_F + |\boldsymbol{\beta} \cdot \boldsymbol{n}| \quad \forall F \in \mathcal{F}_h,$$

with σ_F given in (3).

Provided the exact solution u is regular enough and the stability parameter α in (3) is chosen sufficiently large, the following error estimates hold for the DG solution

$$\begin{aligned} |\!|\!| u - u_h^{\mathrm{DG}} |\!|\!| &\lesssim h^{\ell} \left(\varepsilon^{1/2} + h^{1/2} \|\boldsymbol{\beta}\|_{\infty}^{1/2} \right), \\ \|u - u_h^{\mathrm{DG}}\|_{\mathrm{DG}} &\lesssim h^{\ell} \left(\varepsilon^{1/2} + h^{1/2} \|\boldsymbol{\beta}\|_{\infty}^{1/2} \right). \end{aligned} \tag{8}$$

We refer to [16] and [5] for the proof (in a more general framework) and further details.

For the SUPG method, we define the norm

$$\|v\|_{\mathrm{SUPG}} = \left(\|\varepsilon^{1/2} \nabla v\|_{L^2(\Omega)}^2 + \|v\|_{\boldsymbol{\beta}}^2 \right)^{1/2} \tag{9}$$

for all $v \in V_h^{\mathrm{SUPG}}$. Then, the following estimate holds:

$$\|u - u_h^{\mathrm{SUPG}}\|_{\mathrm{SUPG}} \lesssim h^{\ell} \left(\varepsilon^{1/2} + h^{1/2} \|\boldsymbol{\beta}\|_{\infty}^{1/2} \right), \tag{10}$$

see [24], for example.

Note that the two error estimates (8) and (10) feature the same right hand side (apart from the hidden multiplicative constants).

Remark 4.1. *In the error estimates* (8) *and* (10) *the hidden constants depend on the domain Ω, the shape regularity constant of the partition $\mathcal{T}_h$, and the polynomial approximation degree ℓ, but are independent of the mesh size h and the physical parameters ε and $\boldsymbol{\beta}$ of the problem.*

5 Numerical Results

We compare the numerical performance of the DG and SUPG methods on four test cases. In the first example, we choose a smooth exact solution and compare the approximation properties of the two schemes. In the second and third examples, the exact solutions exhibit an internal and an exponential boundary layer, respectively. Finally, in the last example the (unknown) analytical solution features sharp internal and boundary layers. Throughout this section we set $\Omega = (0,1) \times (0,1)$ and consider a sequence of uniform unstructured triangulations obtained by uniformly refining the initial mesh shown in Figure 2 (left). Denoting by h_0 the mesh size of this initial grid, after $R = 1, 2, \ldots$ refinements the corresponding mesh size is given by $h = h_0/2^R$ (cf. Figure 2 (right), for $R = 2$) . Since the grids are quasi uniform, it holds $h \approx 1/\sqrt{\mathrm{N}}$, N being the number of elements of the partition. Finally, throughout the section, we restrict ourselves to piecewise linear elements, i.e., $\ell = 1$.

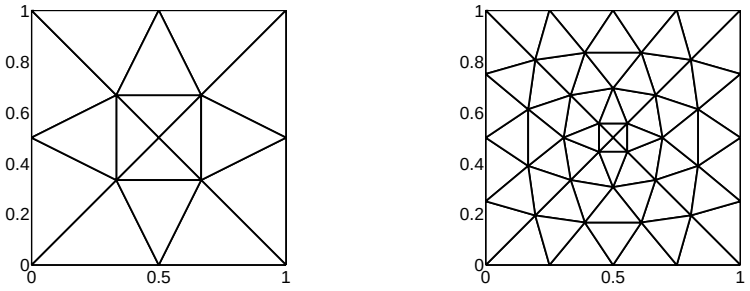

Figure 2: Left: Initial triangulations with mesh size h_0. Right: triangulation obtained after $R = 2$ levels of refinement (mesh size $h_0/4$).

5.1 Example 1

In this section, we aim at comparing the approximation properties of the DG and SUPG schemes on a smooth analytical solution. To this aim, we chose $\boldsymbol{\beta} = (1, 1)^T$, and the source term f such that the solution of problem (1) is $u(x, y) = \sin(2\pi x)(y - y^2)$, for any positive diffusion coefficient ε. Figure 3 (log-log scale) shows the computed errors in the energy norms (7) and (9) versus $1/h$, for different choices of the diffusion coefficient ε, $\varepsilon = 10^{-k}$, $k = 0, 1, 5, 9$. The expected convergence rates are clearly observed: $O(h)$ and $O(h^{3/2})$ convergence rates are attained in the diffusion– and convection–dominated regimes, respectively. We have also compared the errors

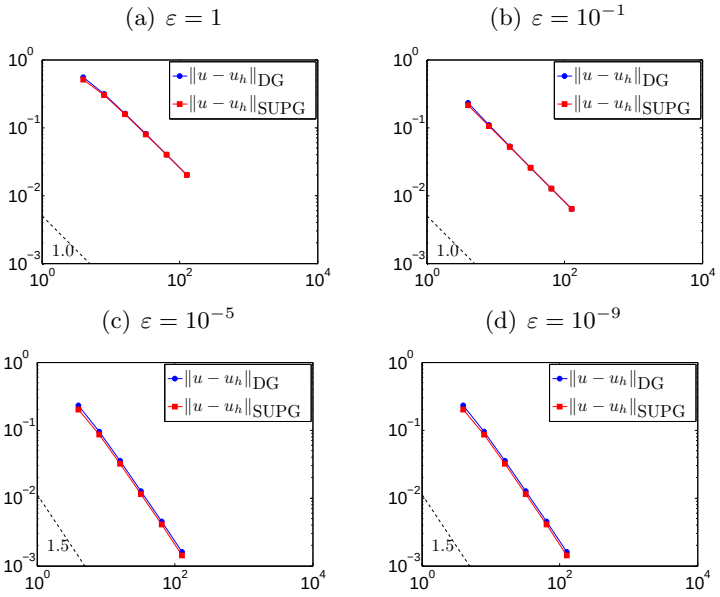

Figure 3: Example 1. Errors in the energy norms (7) and (9) for $\varepsilon = 10^{-k}$, $k = 0, 1, 5, 9$.

computed in the $L^2(\Omega)$ and $L^\infty(\Omega)$ norms. The results are reported in Figure 4 (log-

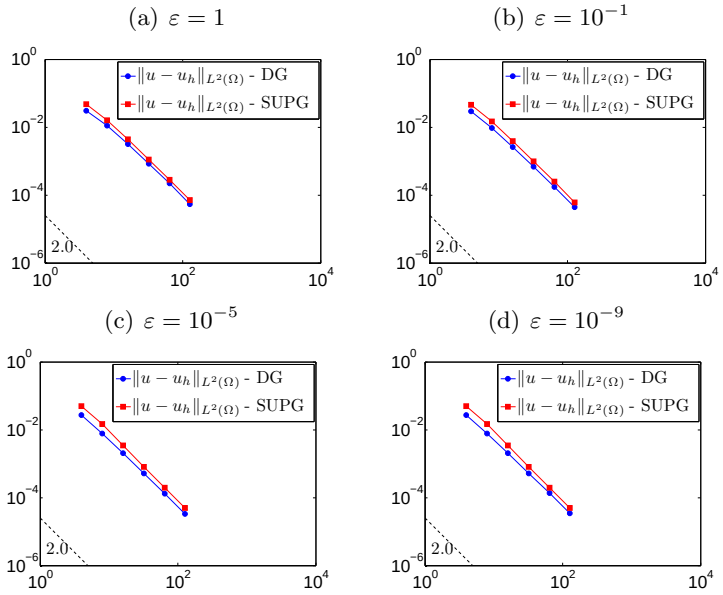

Figure 4: Example 1. Errors in the $L^2(\Omega)$ norm for $\varepsilon = 10^{-k}$, $k = 0, 1, 5, 9$.

log scale) and in Figure 5 (log-log scale), respectively. For all the cases, a quadratic convergence rate is clearly observed, for any value of the diffusion coefficient ε. We have run the same set of experiments on a sequence of structured triangular grids, the results (not reported here, for the sake of brevity) are completely analogous.

From the results reported in Figures 3, 4, 5, we can infer that in the case of a smooth analytical solution, the DG and SUPG enjoy almost the same accuracy, for any value of the diffusion coefficient ε. Indeed, the error curves reported in Figures 3 show that the errors computed in the energy norms (7) and (9) are almost identical. Concerning the error in average (cf. Figure 4) the DG method seems to be slightly more accurate than the SUPG; whereas if we measure the error in the $L^\infty(\Omega)$ norm the SUPG method seems to be slightly better than the DG method (cf. Figure 5). Nevertheless, the difference between the DG and SUPG solutions are negligible, as highlighted by the results reported in Figure 6 where we have plotted, for the same choices of ε, the pointwise absolute value of the difference between the DG and SUPG numerical solutions, on a grid with mesh size $h = h_0/4$.

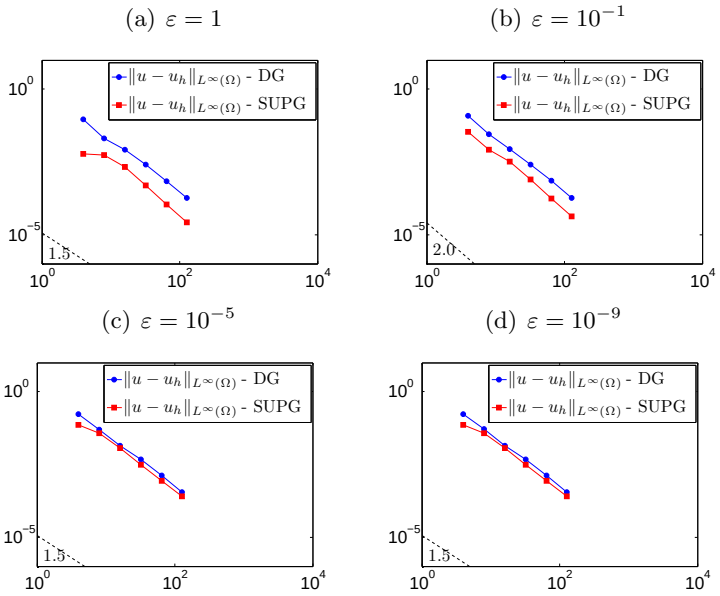

Figure 5: Example 1. Errors in the $L^\infty(\Omega)$ norm for $\varepsilon = 10^{-k}$, $k = 0, 1, 5, 9$.

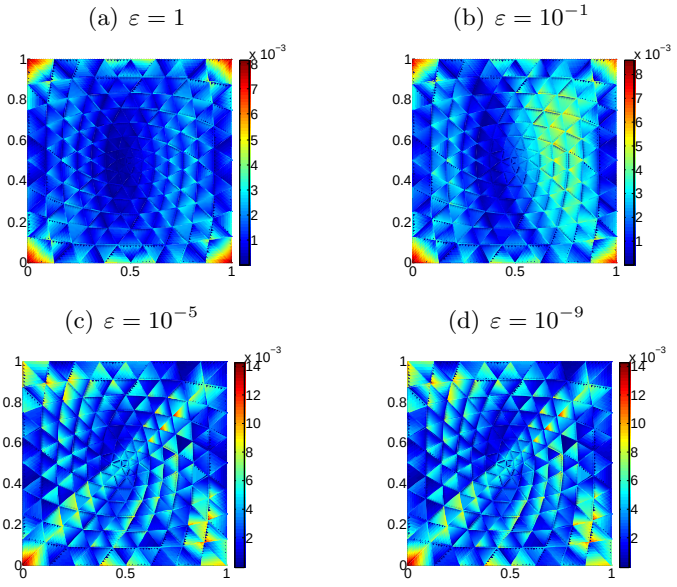

Figure 6: Example 1. Absolute value of the pointwise difference between the DG and SUPG approximate solutions for $\varepsilon = 10^{-k}$, $k = 0, 1, 5, 9$. Grids with mesh sizes $h = h_0/4$.

5.2 Example 2

In the second example, we set again $\boldsymbol{\beta} = (1, 1)$ and let ε vary, however now the exact solution reads

$$u(x, y) = -\text{atan}\left(\frac{(x - 1/2)^2 + (y - 1/2)^2 - 1/16}{\sqrt{\varepsilon}}\right),$$

(the source term f and the non-homogeneous boundary conditions being set accordingly). We notice that, as $\varepsilon \searrow 0^+$, the solution exhibits a sharp internal layer, cf. Figure 7 (left) for $\varepsilon = 10^{-3}$ and Figure 7 (right) for $\varepsilon = 10^{-5}$.

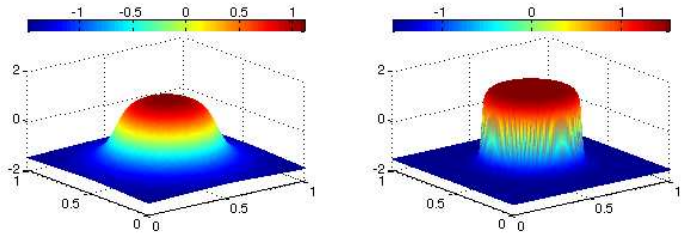

Figure 7: Example 2. Exact solutions for $\varepsilon = 10^{-3}$ (left) and $\varepsilon = 10^{-5}$ (right).

Figure 8 compare the DG and SUPG discrete solutions, respectively, obtained on an unstructured triangular grid of mesh size $h = h_0/4$, for $\varepsilon = 10^{-k}$, $k = 1, 2, 3, 4, 5$. We can observe that the discrete solutions approximate quite well the corresponding analytical solution. Nevertheless, in the convection–dominated regime both methods exhibit spurious oscillations near the internal layer.

We next compare the numerical solutions provided by the two methods. In Figure 9 the pointwise absolute error of the DG and SUPG approximate solutions is reported on a grid with mesh size $h = h_0/4$, for $\varepsilon = 10^{-k}$, $k = 1, 2, 3, 4, 5$. Notice that, in this case, the approximate solutions provided by the two methods are almost identical in the diffusion–dominated regime (cf. Figure 9, top), whereas they differ substantially near the internal layer in the convection–dominated regime (cf. Figure 9, bottom). Indeed, as ε becomes small, they both exhibit oscillations near the internal layer, but of different kind.

Finally, for $\varepsilon = 10^{-k}$, $k = 1, 2, 3, 4$, Figure 10 (log-log scale) and Figure 11 (log-log scale) show the computed errors in the energy norms (7) and (9) and in the $L^2(\Omega)$ norm, respectively. The results reported in Figure 10 and Figure 11 have been obtained on unstructured triangular grids as the ones shown in Figure 2; analogous results (not reported here) have been obtained on structured triangular grids and the same convergence behavior has been observed. The error in the energy norms goes to zero at the predicted rate, namely linearly in the diffusion–dominated case and at a rate of 3/2 in the convection–dominated regime. Nevertheless, notice that such a rate seems to be achieved only asymptotically for $\varepsilon = 10^{-4}$ by both the DG and SUPG methods. Concerning the mean error (cf. Figure 11), we observe that both methods achieve a quadratic convergence rate, and the DG scheme seems to be slightly more accurate than the SUPG method. If we measure the errors in the $L^\infty(\Omega)$ norm (cf. Figure 12) we observe again a quadratic convergence rate but in this case the SUPG method seems to be slightly more accurate.

(a) $\varepsilon = 10^{-1}$

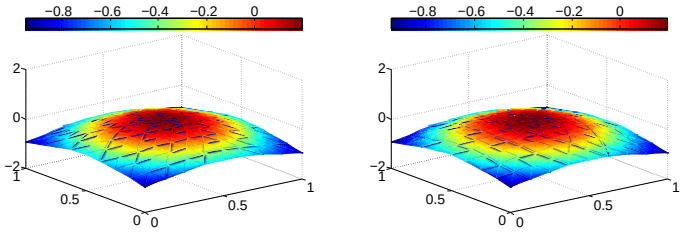

(b) $\varepsilon = 10^{-2}$

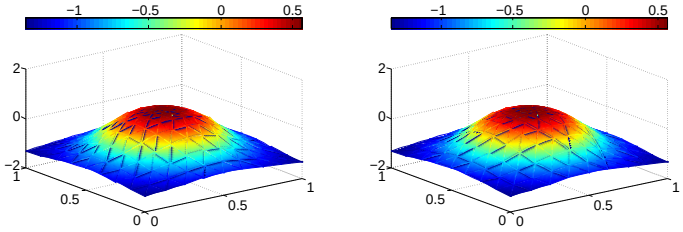

(c) $\varepsilon = 10^{-3}$

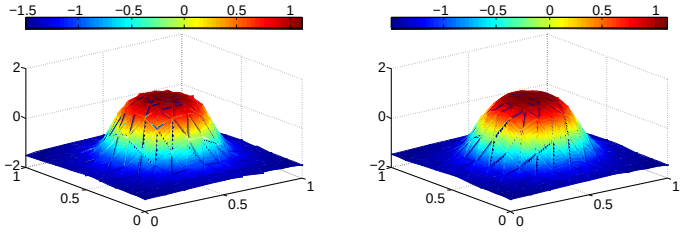

(d) $\varepsilon = 10^{-4}$

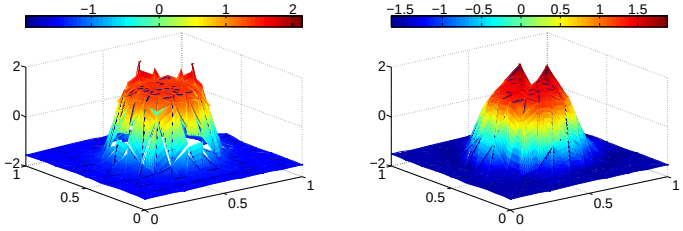

(e) $\varepsilon = 10^{-5}$

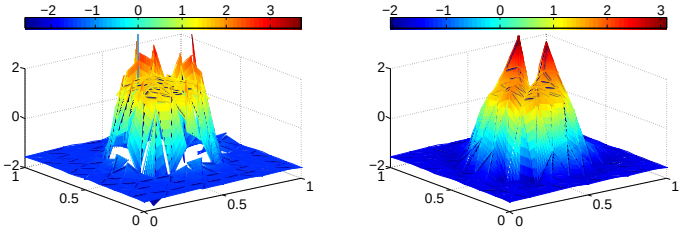

Figure 8: Example 2. DG (left) and SUPG (right) approximate solutions on an grid of mesh size $h = h_0/4$ for $\varepsilon = 10^{-k}$, $k = 1, 2, 3, 4, 5$.

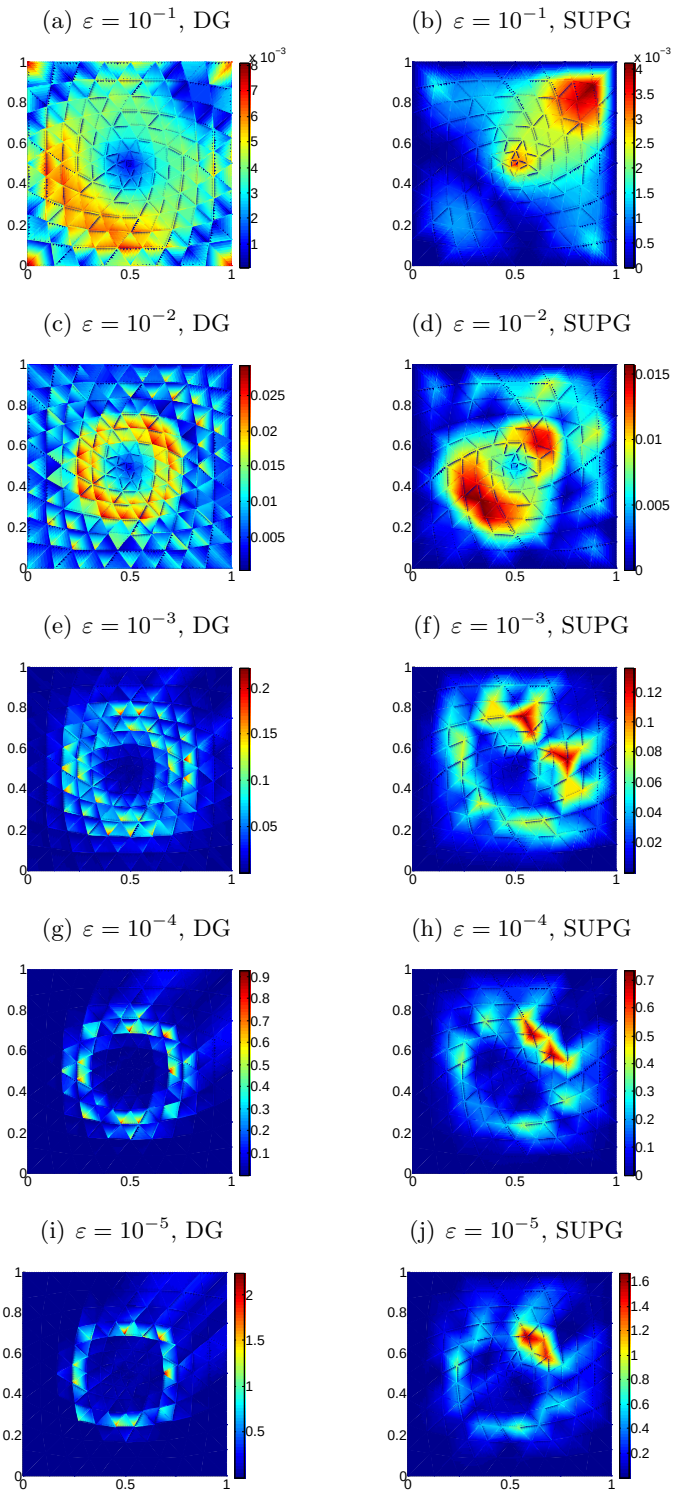

Figure 9: Example 2. Pointwise absolute error of the DG and SUPG approximate solutions for $\varepsilon = 10^{-k}$, $k = 1, 2, 3, 4, 5$. Mesh size $h = h_0/4$.

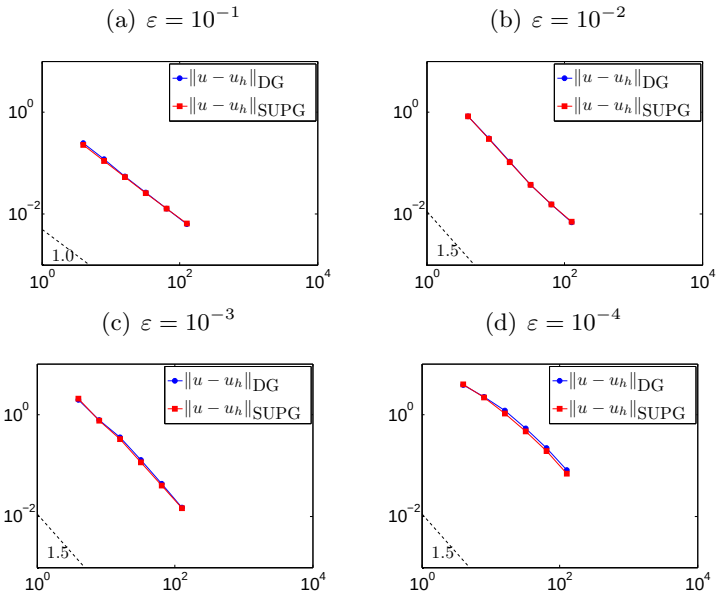

Figure 10: Example 2. Errors in the energy norms for $\varepsilon = 10^{-k}$, $k = 1, 2, 3, 4$.

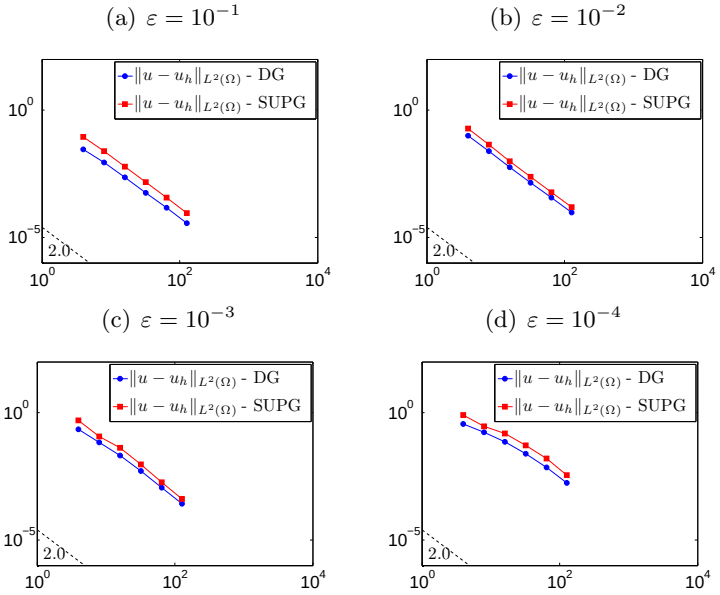

Figure 11: Example 2. Errors in the $L^2(\Omega)$ norm for $\varepsilon = 10^{-k}$, $k = 1, 2, 3, 4$.

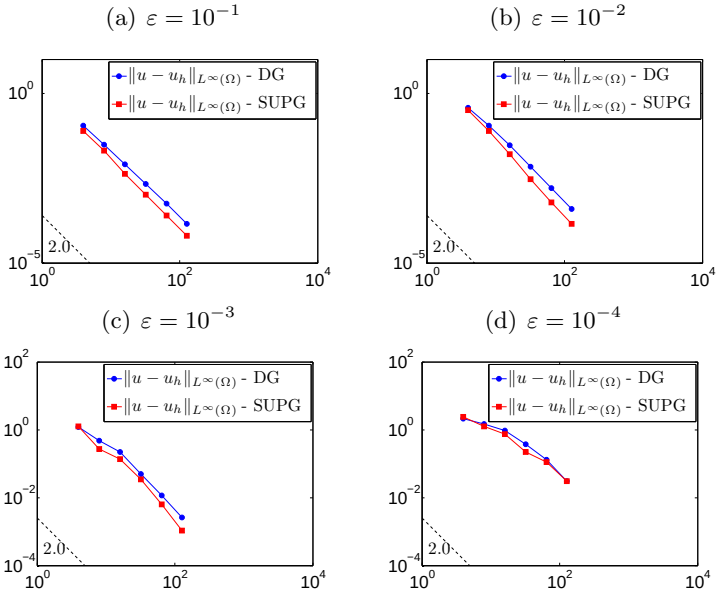

Figure 12: Example 2. Errors in the $L^\infty(\Omega)$ norm for $\varepsilon = 10^{-k}$, $k = 1, 2, 3, 4$.

5.3 Example 3

In this example, we consider a test case with an exponential boundary layer taken from [16] and [5], which is the multi-dimensional version of the one-dimensional test proposed by [23]. We set $\boldsymbol{\beta} = (1, 1)$, and vary the diffusion coefficient ε. The right hand side f and the non-homogeneous boundary condition are chosen in such a way that the exact solution is given by:

$$u(x, y) = x + y - xy + \frac{\mathrm{e}^{-1/\varepsilon} - \mathrm{e}^{-(1-x)(1-y)/\varepsilon}}{1 - \mathrm{e}^{-1/\varepsilon}}.$$

Figure 13 shows the discrete solutions computed with the DG and SUPG methods for $\varepsilon = 10^{-k}$, $k = 0, 1, 2, 9$ on a grid with mesh size $h = h_0/4$. We can observe that, for $\varepsilon = 1, 10^{-1}$ the two solutions are almost identical, whereas in the intermediate regime $\varepsilon = 10^{-2}$ the DG method exhibits some spurious oscillations near the boundary layer, while the SUPG solution seems to be definitely more accurate. Finally, we observe that in the convection–dominated regime, the DG solution is totally free of spurious oscillations but the boundary layer is not captured. Such a behavior, already observed in [5], is due to the fact that the boundary conditions are imposed weakly. On the other hand, for $\varepsilon = 10^{-9}$ the SUPG method results in overshoot near the point $(1, 1)$. The above considerations are also confirmed by the results reported in Figure 14 where the absolute value of the pointwise error is shown on grid with mesh size $h = h_0/4$.

Finally, Figure 15 shows the computed errors in the $L^2(\Omega)$ and $L^1(\Omega)$ norms for $\varepsilon = 10^{-k}$, $k = 0, 1, 9$. In the diffusion–dominated regime and for both the methods the errors go to zero quadratically as the mesh is refined, whereas for $\varepsilon = 10^{-9}$ the DG method is quadratically convergent in both the $L^2(\Omega)$ and $L^1(\Omega)$ norm while

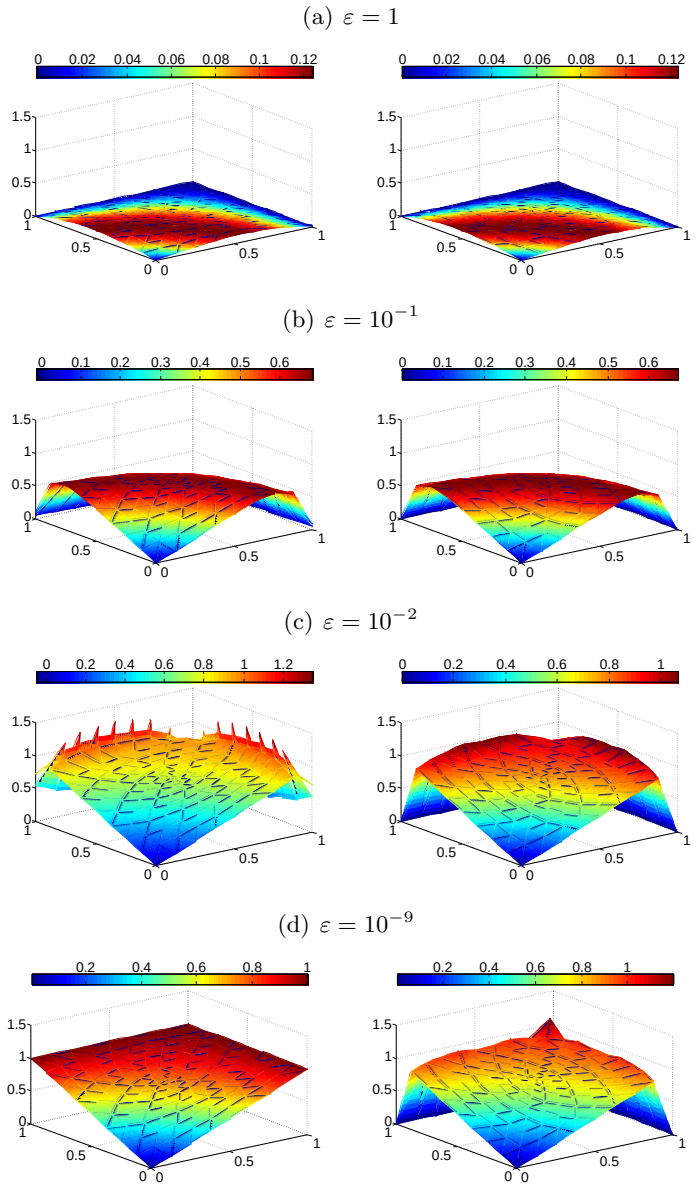

Figure 13: Example 3. DG (left) and SUPG (right) discrete solutions for $\varepsilon = 10^{-k}$ $k = 0, 1, 2, 9$. Mesh size $h = h_0/4$.

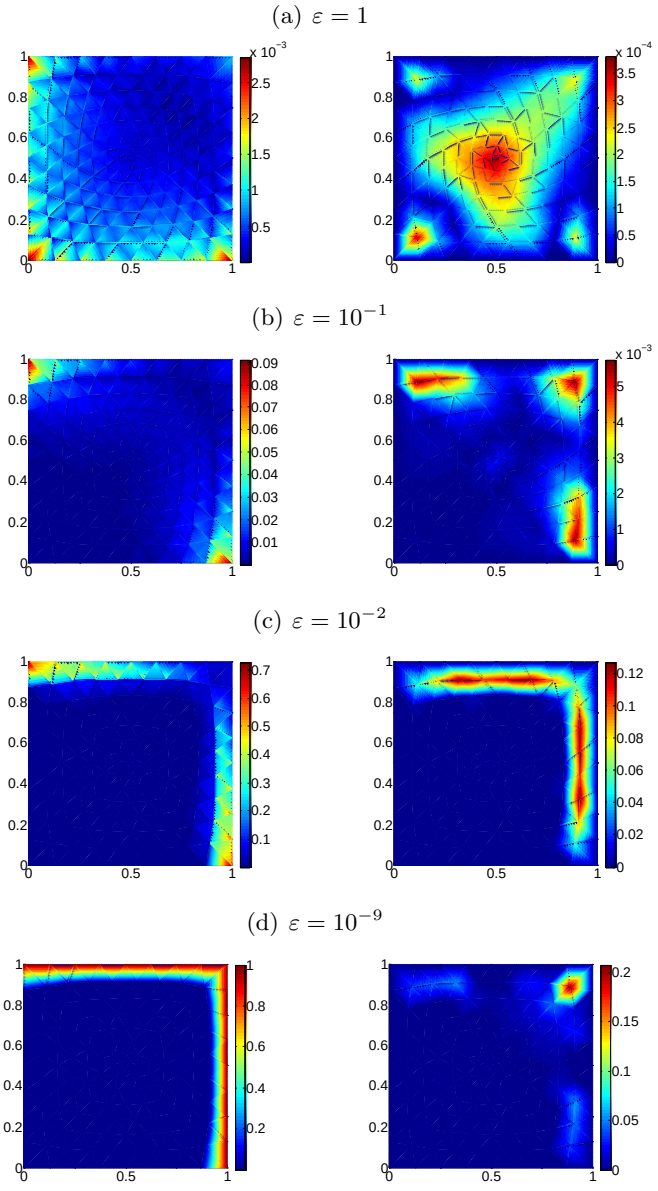

Figure 14: Example 3. Pointwise absolute error of the DG and SUPG approximate solutions for $\varepsilon = 10^{-k}$, $k = 0, 1, 2, 9$. Mesh size $h = h_0/4$.

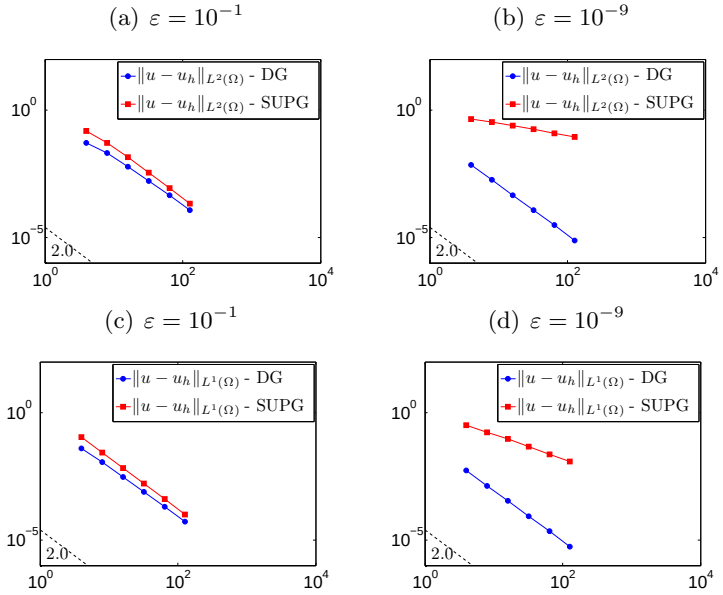

Figure 15: Example 3. Errors in the $L^2(\Omega)$ (top) and $L^1(\Omega)$ (bottom) norms for $\varepsilon = 10^{-k}$, $k = 1, 9$.

the SUPG method convergences at a rate of order $O(h^{1/2})$ and $O(h)$ in the $L^2(\Omega)$ and $L^1(\Omega)$ norms, respectively.

5.4 Example 4

In the last example, always with $\Omega = (0,1)^2$, we consider the following convection–diffusion equation:

$$-\varepsilon\Delta u + \boldsymbol{\beta}\cdot\nabla u \quad = 0 \quad \text{in } \Omega, \quad u = g \quad \text{on } \partial\Omega.$$

The Dirichlet boundary conditions are set as follows:

$$g = \begin{cases} 1 & \text{if } y = 0, \\ 1 & \text{if } x = 0 \text{ and } y \leq 1/2, \\ 0 & \text{otherwise,} \end{cases}$$

the velocity $\boldsymbol{\beta}$ is chosen as $\boldsymbol{\beta} = (\cos(\pi/3), \sin(\pi/3))$, and we let ε vary. Notice that in this case, a close expression for the exact solution is not available. We know however that, as ε tends to zero, the exact solution exhibits a strong internal and boundary layer.

We compare the discrete solutions computed by the DG and SUPG schemes for $\varepsilon = 10^{-k}$, $k = 0, 3, 9$. The results on the unstructured triangular mesh with mesh size $h = h_0/8$ are shown in Figure 16. The following conclusions can be drawn:

i) in the diffusion–dominated regime, the DG and SUPG methods are substantially equivalent;

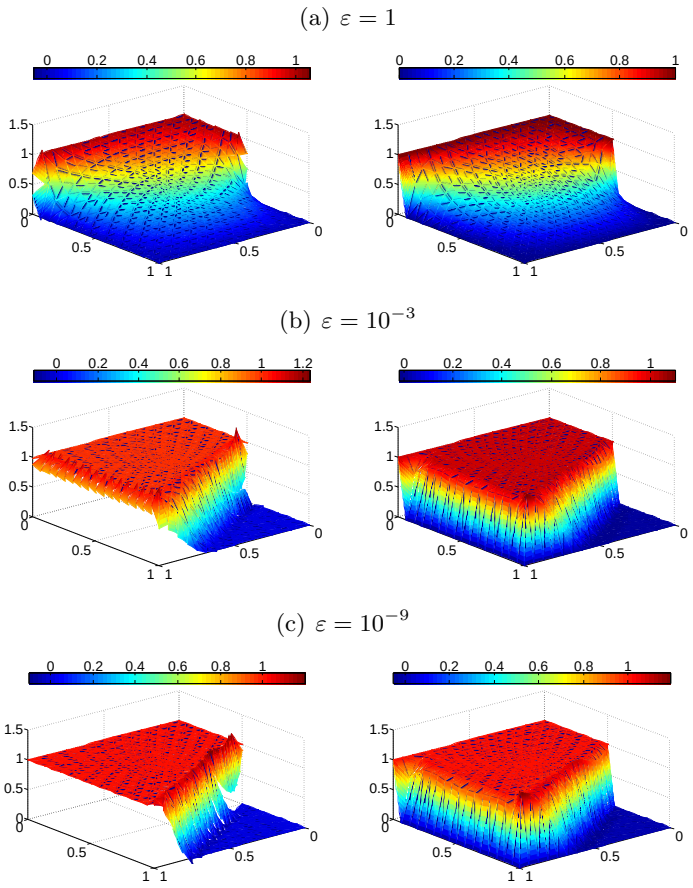

Figure 16: Example 4. DG (left) and SUPG (right) discrete solutions for $\varepsilon = 10^{-k}$, $k = 0, 3, 9$. Mesh size $h = h_0/8$.

ii) in the intermediate regime, the DG method exhibits spurious oscillations, whereas the SUPG method seems to be more stable and only an overshooting effect is observed near the point $(1, 1)$;

iii) in the convection–dominated regime, DG method exhibits some spurious oscillations on the internal layer whereas no oscillations along boundary layer are present, however unfortunately the boundary layer is completely missed. On the other hand SUPG method exhibits again an overshooting phenomenon near the point $(1, 1)$ and also some spurious oscillations along the internal layer.

The above considerations are also confirmed by the results reported in Figure 17 where the absolute value of the pointwise difference between the DG and SUPG approximate solutions for $\varepsilon = 10^{-k}$, $k = 0, 3, 9$, are reported. Results shown in Figure 17 (left) have been obtained on a grid with mesh size $h = h_0/8$; the analogous ones obtained on a finer triangulation with mesh size $h = h_0/16$ are reported in Figure 17 (right).

(a) $\varepsilon = 1$

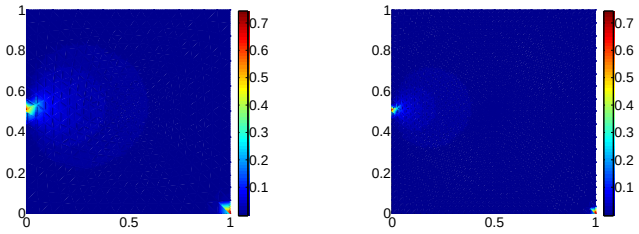

(b) $\varepsilon = 10^{-3}$

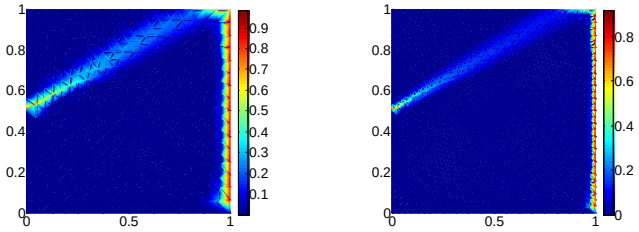

(c) $\varepsilon = 10^{-9}$

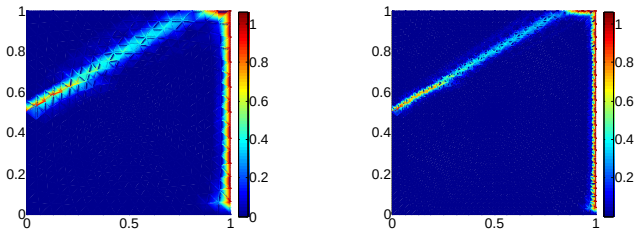

Figure 17: Example 4. Pointwise absolute difference between the DG and SUPG approximate solutions for $\varepsilon = 10^{-k}$, $k = 0, 3, 9$. Mesh size $h = h_0/8$ (left) and $h = h_0/16$ (right).

6 Conclusions

In this paper we have recalled the formulation and principal properties of DG and SUPG approximations of linear steady–state convection–diffusion equations. The aim was to carry out a careful comparison of their performance (as of stability, accuracy and numerical robustness) in three different solution regimes: diffusion–dominated, intermediate, and convection– dominated. Our comparative analysis is made for piecewise linear elements on a number of significant test problems. As expected, DG and SUPG methods are substantially equivalent in the diffusion–dominated regime. In the intermediate regime, SUPG looks more robust (even if overshooting may occur in the boundary layer). In the convection–dominated regime, SUPG still exhibits overshooting whereas DG is oscillation free, at least when the exact solution features sharp boundary layers. However, it is fair to notice that the DG method is not able to capture the boundary layers (indeed, the latter are completely missed because of the weak enforcement of boundary conditions). An in depth comparison between discontinuous and stabilized continuous Galerkin methods in the case of higher order polynomial approximations and transient convection–diffusion problems is currently under investigation [2].

Acknowledgements

P.F.A. has been partially supported by Italian MIUR PRIN 2008 “Analisi e sviluppo di metodi numerici avanzati per EDP”. A.Q. acknowledges the financial support of Italian MIUR PRIN 2009 “Modelli numerici per il calcolo scientifico e applicazioni avanzate”.

References

[1] P. F. Antonietti and P. Houston. A pre-processing moving mesh method for discontinuous Galerkin approximations of advection-diffusion-reaction problems. *Int. J. Numer. Anal. Model.*, 5(4):704–728, 2008.

[2] P. F. Antonietti and A. Quarteroni. In preparation. 2011.

[3] D. N. Arnold. An interior penalty finite element method with discontinuous elements. *SIAM J. Numer. Anal.*, 19(4):742–760, 1982.

[4] D. N. Arnold, F. Brezzi, B. Cockburn, and L. D. Marini. Unified analysis of discontinuous Galerkin methods for elliptic problems. *SIAM J. Numer. Anal.*, 39(5):1749–1779 (electronic), 2002.

[5] B. Ayuso de Dios and L. D. Marini. Discontinuous Galerkin methods for advection-diffusion-reaction problems. *SIAM J. Numer. Anal.*, 47(2):1391–1420, 2009.

[6] C. E. Baumann and J. T. Oden. A discontinuous *hp* finite element method for convection-diffusion problems. *Comput. Methods Appl. Mech. Engrg.*, 175(3-4):311–341, 1999.

[7] F. Brezzi, L. D. Marini, and E. Süli. Discontinuous Galerkin methods for first-order hyperbolic problems. *Math. Models Methods Appl. Sci.*, 14(12):1893–1903, 2004.

[8] A. N. Brooks and T. J. R. Hughes. Streamline upwind/Petrov-Galerkin formulations for convection dominated flows with particular emphasis on the incompressible Navier-Stokes equations. *Comput. Methods Appl. Mech. Engrg.*, 32(1-3):199–259, 1982. FENOMECH '81, Part I (Stuttgart, 1981).

[9] A. Buffa, T. Hughes, and G. Sangalli. Analysis of a multiscale discontinuous galerkin method for convection diffusion problems. *SIAM J. Numer. Anal.*, 44(4):1420–1440, 2006.

[10] E. Burman and G. Smith. Analysis of the space semi-discretized supg-method for transient convection–diffusion equations, 2010. Mathematical Models and Methods in Applied Sciences, DOI 10.1142/S0218202511005659.

[11] I. Christie, D. F. Griffiths, A. R. Mitchell, and O. C. Zienkiewicz. Finite element methods for second order differential equations with significant first derivatives. *IJNME*, 10(6):1389–1396, 1976.

[12] B. Cockburn. Discontinuous Galerkin methods for convection-dominated problems. In *High-order methods for computational physics*, volume 9 of *Lect. Notes Comput. Sci. Eng.*, pages 69–224. Springer, Berlin, 1999.

[13] J. Douglas, Jr. and T. Dupont. Interior penalty procedures for elliptic and parabolic Galerkin methods. In *Computing methods in applied sciences (Second Internat. Sympos., Versailles, 1975)*, pages 207–216. Lecture Notes in Phys., Vol. 58. Springer, Berlin, 1976.

[14] J. H. Ferziger and M. Perić. *Computational methods for fluid dynamics*. Springer-Verlag, Berlin, revised edition, 1999.

[15] L. Franca, I. Harari, and S. Olivera. Streamline design of stability parameters for advection–diffusion problems. *J. Comput. Phys.*, 171:115–131, 2001.

[16] P. Houston, C. Schwab, and E. Süli. Discontinuous *hp*-finite element methods for advection-diffusion-reaction problems. *SIAM J. Numer. Anal.*, 39(6):2133–2163 (electronic), 2002.

[17] V. John and P. Knobloch. On spurious oscillations at layers diminishing (SOLD) methods for convection-diffusion equations. I. A review. *Comput. Methods Appl. Mech. Engrg.*, 196(17-20):2197–2215, 2007.

[18] V. John and P. Knobloch. On spurious oscillations at layers diminishing (SOLD) methods for convection-diffusion equations. II. Analysis for P_1 and Q_1 finite elements. *Comput. Methods Appl. Mech. Engrg.*, 197(21-24):1997–2014, 2008.

[19] C. Johnson, U. Nävert, and J. Pitkäranta. Finite element methods for linear hyperbolic problems. *Comput. Methods Appl. Mech. Engrg.*, 45(1-3):285–312, 1984.

[20] R. J. LeVeque. *Finite volume methods for hyperbolic problems*. Cambridge Texts in Applied Mathematics. Cambridge University Press, Cambridge, 2002.

[21] R. J. LeVeque. *Finite difference methods for ordinary and partial differential equations*. Society for Industrial and Applied Mathematics (SIAM), Philadelphia, PA, 2007. Steady-state and time-dependent problems.

[22] J. Liesen and Z. Strakos. Gmres convergence analysis for a convection-diffusion model problem. *SIAM J. on Scientific Computing*, 26:1989–2009, 2005.

[23] J. M. Melenk and C. Schwab. An *hp* finite element method for convection-diffusion problems in one dimension. *IMA Journal of Numerical Analysis*, 19(3):425–453, 1999.

[24] A. Quarteroni and A. Valli. *Numerical approximation of partial differential equations*, volume 23 of *Springer Series in Computational Mathematics*. Springer-Verlag, Berlin, 1994.

[25] W. Reed and T. Hill. Triangular mesh methods for the neutron transport equation. Technical Report Tech. Report LA-UR-73-479, Los Alamos Scientific Laboratory, 1973.

[26] H.-G. Roos, M. Stynes, and L. Tobiska. *Numerical methods for singularly perturbed differential equations: convection-diffusion and flow problems*. Springer Verlag, Berlin, 1996.

MOX Technical Reports, last issues

Dipartimento di Matematica "F. Brioschi",
Politecnico di Milano, Via Bonardi 9 - 20133 Milano (Italy)

42/2011 Antonietti, P.F.; Quarteroni, A.
Numerical performance of discontinuous and stabilized continuous Galerkin methods or convection-diffusion problems

41/2011 Burman, E.; Zunino, P.;
Numerical Approximation of Large Contrast Problems with the Unfitted Nitsche Method

40/2011 D Angelo, C.; Zunino, P.; Porpora, A.; Morlacchi, S.; Migliavacca, F.
Model reduction strategies enable computational analysis of controlled drug release from cardiovascular stents

39/2011 Antonietti, P.F.; Ayuso de Dios, B.; Brenner, S.C.; Sung, L.-Y.
Schwarz methods for a preconditioned WOPSIP method for elliptic problems

38/2011 Porpora A., Zunino P., Vergara C., Piccinelli M.
Numerical treatment of boundary conditions to replace lateral branches in haemodynamics

37/2011 Ieva, F.; Paganoni, A.M.
Depth Measures For Multivariate Functional Data

36/2011 Motamed, M.; Nobile, F.; Tempone, R.
A stochastic collocation method for the second order wave equation with a discontinuous random speed

35/2011 Iapichino, L.; Quarteroni, A.; Rozza, G.
A Reduced Basis Hybrid Method for the coupling of parametrized domains represented by fluidic networks

34/2011 Benacchio, T.; Bonaventura, L.
A spectral collocation method for the one dimensional shallow water equations on semi-infinite domains

33/2011 Antonietti, P.F.; Beirao da Veiga, L.; Lovadina, C.; Verani, M.

Hierarchical a posteriori error estimators for the mimetic discretization of elliptic problems